Identification of key pathways and hub genes in the myogenic differentiation of pluripotent stem cell: A bioinformatics and experimental study

Wenyong Fei
Yangzhou University Medical Academy
Mingsheng Liu
Dalian Medical University
Yao Zhang
Dalian Medical University
Shichao Cao
Dalian Medical University
Xuanqi Wang
Dalian Medical University
Bin Xie
Dalian Medical University
Jingcheng Wang (jingchengwang123@163.com)
Yangzhou University Medical Academy

Research article

Keywords: stem cells, muscular regeneration, MyoD, actin, bioinformatics analysis

Posted Date: September 11th, 2020

DOI: https://doi.org/10.21203/rs.3.rs-41291/v2

Version of Record: A version of this preprint was published on January 4th, 2021. See the published version at https://doi.org/10.1186/s13018-020-01979-x.

Abstract

Background: The regeneration of muscle cells from stem cells is an intricate process and various genes are included in the process as myoD, mf5, mf6 etc. The key genes and pathways in the differentiating stages is various. Therefore, the differential expression of key genes after 4weeks of differentiation were investigated in our study. Method: Three published gene expression profiles, GSE131125, GSE148994, GSE149055, about the comparisons of pluripotent stem cells to differentiated cells after 4 weeks were obtained from the Gene Expression Omnibus (GEO) database. Common differentially expressed genes (DEGs) were obtained for further analysis as proteinprotein interaction (PPI) network, Gene Ontology (GO), Kyoto Encyclopedia of Genes and Genomes (KEGG) and GSEA analysis. After hub genes and key pathways were obtained, we manipulated in vitro cell research for substantiation as immunohistochemical staining and semi-quantitative analysis and quantitative real-time PCR. Results: A total of 824 DEGs including 350 up-regulated genes and 474 down-regulated genes were identified in the three GSEs. 19 hub genes were identified from the PPI network. The GO and KEGG pathway analysis confirmed that myogenic differentiation at 4 weeks was strongly associated with pathway in cancer, PI3K pathway, actin cytoskeleton regulation and metabolic pathway, biosynthesis of antibodies and cell cycle. GSEA analysis indicated the differentiated cells were enriched in muscle cell development and myogenesis. Meanwhile, the core genes in each pathway were identified from the GSEA analysis. The in vitro cell research revealed that actin cytoskeleton and myoD were up-regulated after 4 weeks differentiation. Conclusions: The research revealed the potential hub genes and key pathways after 4 weeks differentiation of stem cells which contribute to further study about the molecular mechanism of myogenesis regeneration. Paving a way for more accurate treatment for muscle dysfunction.

Introduction

As the aging of human population, muscle dysfunction has been an interrupting issue in clinical research.[1-4] A series of diseases were correlated to the atrophy of skeletal muscles and leading to dysfunction of muscular organs as Duchenne muscular dystrophy (DMD), degenerative rotator cuff tear etc.[5-7] Stem cells are promising cells that have the potency of multi-directional differentiation and proliferation and are widely expected to be used in the field of tissue repair and regeneration[8, 9]. In the muscle regeneration field, stem cells also showed vigorous potency.[10]

Various researches have devoted to verifying the mechanism of myoblast differentiation. Myogenic differentiation as a multistage process, there stays several regulating factors as Myf5, Myf6, myoD and myog[11-13]. Meanwhile, researches have shown that different factors were correlate with different stages at the myogenic process as myoD at the late stage and myf5 at the early stage[14,15,16]. What is more, couples of pathways were verified to be correlated to myogenic differentiation as PI3K-MAPK, p38, p53 and actin pathway[14-17], but few researches have shown the pathways variation at differentiation stages. To up-regulate the differentiation efficacy and contribute to the repair of degenerated muscular tissues, it is especially important to clarify the differentiation mechanism at genetic level.

With the wide spread use and development of high-throughput sequencing, bioinformatics analysis showed great advantage for determining the myogenic differentiation mechanism of stem cell at genetic level. However, no study was designed to integrate the myogenic differentiation datasets in GEO. In the present study, we integrated 3 datasets in GEO comparing human pluri-potential stem cells and myogenic stem cells. Bioinformatics analysis was used to explore molecular mechanism of the pathogenesis in myogenic differentiation of stem cells.

Materials And Methods

Microarray data obtained:

Three gene expression profiles, GSE131125(GPL 20844, SurePrint G3 Human GE v3 8x60K Microarray 039494), GSE148994 and GSE149055(GPL16686, Affymetrix Human Gene 2.0 ST Array) were obtained from the GEO database. Both the GSE149055 and GSE148994 contained 6 samples, of which 3 were undifferentiated stem cells and 3 were differentiated cells after 30 days differentiation. GSE133125 contained 24 samples which include different time-point of the differentiation. We choose the 3 undifferentiated stem cells and 3 differentiated for 25 days into our analysis.

Identification of differently expressed genes (DEGs)

The downloaded platform files were matched to the gene expression profiles by the “VLOOKUP” function of Excel 2010. Gene differential analysis was determined to summarized the differentially expressed genes (DEGs). The DEGs threshold of our study was |logFC|>1 and adj.P-value<0.01. Heatmaps of DEGs from 3 groups were generated by graphpad 8.0.2. Online tool Venn, version 2.1(bioinformatics.psb.ugent.be/webtools/Venn;version 2.1) was used to determine the common DEGs among the three profiles.

(Protein-protein interaction) PPI network construction and module selection

Search Tool for the Retrieval Interacting Genes (STRING) database was used to construct the network of differentially expressed genes and proteins and Molecular Complex Detection (MCODE; version 1.31) in the Cytoscape (version 3.8.0) was used to analysis modules in the network.

GO and pathway enrichment analysis construction

Both the GO and KEGG analysis was applied under the online program Database for Annotation, Visualization and Integrated Discovery (DAVID, version 6.8) whose subgroup of functional annotation tools can help the researchers to understand the biological meanings about the selected genes. Gene Set Enrichment Analysis (version 4.0.3) was used to verify whether DEGs Showed statistical significance in one phenotype or pathway based on the expression profiles.

Isolation and cultivation of ADSCs

An eight-week-old New Zealand white rabbit (Animal Experiment Center of Jiangsu University) weighing 2.0 kg was sacrificed under the guidelines of the Institutional Animal Care and Use Committee of Jiangsu University, China. The rabbit was kept and fed in a single cage in housing conditions. Housing was controlled in temperature (25°C)，humidity (40– 60%) and light (12 h, light–dark cycle). Animals were observed for one week before surgery to confirm that they were healthy and disease-free.

0.6 % sodium pentobarbital (4 mg/ kg) was injected into the rabbits' ear veins for general anesthesia. Then 2 % lidocaine hydrochloride was injected into the planned skin incision to enhance the effect of anesthesia. Priority to placing the animals in a laminar flow chamber, the hair was clipped at the abdominal area. An incision was made along with the linea alba to expose the peritoneum, and the inguinal fat was removed.

The adipose tissue was washed three times with phosphate-buffered saline (PBS) to remove red blood cells. The collected adipose tissue was cut into small pieces and transferred into one 20 mL centrifuge tube, and an equal volume of a 0.25% trypsin (Gibco, USA) and 0.1% type I collagenase (Sigma, USA) mixture was added. The tissue was incubated on shaking tables at 37°C with constant agitation for approximately 15 minutes. Afterwards, the liquid was separated into three layers: the upper layer contained yellow oily lipocytes, the intermediate layer contained adipose tissue, and the bottom layer contained mononuclear cells. The bottom layer was extracted and transferred into a centrifuge tube containing 15% fetal bovine serum (FBS, Gibco, USA) and high-glucose DMEM (Sigma, USA). The remaining stromal fractions were treated with 3 mL red blood cell lysis buffer (Sigma, USA) for 10 minutes at room temperature, filtered through a 100-mm nylon mesh, and centrifuged at 1200 ×g for 10 minutes; then, the supernatant was removed. The cell pellets were then suspended in high-glucose DMEM containing 15% FBS (Gibco Company, St. Louis, MO, USA), 100 U/mL penicillin, and 100 mg/mL streptomycin (Gibco Company, St. Louis, MO, USA). The cells were cultured at 37°C and 5.0% CO2 in a humidified incubator, with full media replacement every 3 days. When the cells reached 80% confluence, they were digested with a mixture of 0.25% trypsin and 0.04% EDTA (Shanghai Reagent, China) and passaged for later use.

Flow cytometry（FCM）analysis of ADSCs

Passage-3 adherent cells were treated with 0.25% trypsin (Gibco, USA) and washed twice with PBS. The cells were incubated with rabbit anti-CD45, anti-CD90 antibodies (Invitrogen, USA, and Gibco, USA) overnight at 4°C. Unbound antibodies were removed by washing three times with PBS. After washing, the cells were incubated for 45 minutes at room temperature in the dark with Cy3-labeled secondary anti-goat/anti-rabbit antibody and resuspended in PBS for FACS analysis. At least 1×10^6 cells per sample were analyzed with a flow cytometer (BD FACSVerse, USA). CELLQuest software was used for the analysis.

Assessment of cell viability by tetrazolium method （MTT）

The cell viability was quantitatively determined by the Tetrazolium (MTT) method. MTT is a yellow tetrazolium dye which responds to metabolic activity. The reductases in living cells reduce MTT from a pale-yellow compound to dark-blue formazan crystals. The passage-3 ADSCs were digested and diluted, and the mixture was transferred to a 96-well culture plate (Thermo Scientific, USA) at 1×10^5 cells per well. 5-Aza was then added to each well at concentrations of 0, 10, 20, 30, 40 μmol/l. Then, at 24h, 48 and 72 hours after induction, the absorbance which represent cell viability was tested in each group. Firstly, the supernatant was removed. Then, 200 μL of dimethyl sulfoxide (DMSO, Merck, Germany) was added to each well to dissolve the blue substance. Finally, the absorbance (OD) at 570 nm was read using a microplate reader (Biotek, USA).

Induction of differentiation of ADSCs by 5-Azacytidine(5-Aza)

The passage 3 ADSCs were digested by a mixture of trypsin and EDTA and dilutaed to single-cell suspension of 10^4 cells/mL and then seeded into cell culture flasks. Group A, B and C were induced by 0, 10, and 20 μmol/L 5-Aza (Sigma, USA) for 24hours and washed with D-Hanks balanced salt solution (HBSS, Gibco Company, St. Louis, MO, USA). Then, the medium was replaced with low-glucose DMEM containing 10% FBS. The cells in each group were incubated at 37°C with 5% CO2 in conventional incubator. The medium was replaced with fresh DMEM and FBS every 3 days until the test begin after 25 days cultivation.

Immunohistochemical staining and Semi-quantitative analysis

We determined the KEGG pathway of actin cytoskeleton about expression of actin by immunohistochemical staining. The cells were digested and diluted 25 days after induction and added 150μl 4% paraformaldehyde fixative to every slide and left them undisturbed for 30 minutes before adding 150μl 0.1% Triton x-100microplate reader (Biotek, USA). Primary antibody α-SMA (1:200) (Proteintech, USA), secondary antibody (1:200) (Proteintech, USA) and Hoechst33258 stain (C1011 Beyotine, China) was added to each slide in a dark environment at room temperature. Finally, we observed the cells under a fluorescence microscop e(Leica, Germany), photographed, and stored them. ImageJ (Rawak Software, Germany) software was used for photography and Prism Demo software for data statistics (GraphPad Software, USA).

Quantitative real-time PCR

Total RNA was extracted from the ADSCs after induction of 25 days using Trizol lysate （invitrogen）. The schizolytic cells were then transferred into another tube without RNA enzymes, and 200 μl pre-cooling chloroform (Sigma Centrifuge, Germany) was added per milliliter of Trizol. The ccentrifugation yielded RNA sediments that were preserved in a -20℃ surrounding for 30 minutes. The sediments were washed with 75% ethyl alcohol and centrifuged for 5 minutes, and the supernatant was discarded after washing and centrifuging the sediments twice. The reverse transcription system was prepared using a reverse transcription kit (Thermo Scientific, USA) according to instructions provided in the protocol of the kit.

Statistical analysis

Statistical analysis was performed on Graphpad 8.0.2 and R 4.0.0. Expressed data were shown as mean±SD. Student's t test was used to evaluate the statistical significance of different 3 groups. P value less than 0.05 was considered as significant.

Results

Identification of DEGs

The three datasets were standardized and the results are shown in Figure1. The threshold of DEGs determination was that |LOG(FC)| lower than 1 and adj.P.Value lower than 0.01. From the GSE131125 database, there were 5051 up-regulated and 5199 down-regulated DEGs. Meanwhile, 864 up-regulated and 1038 down-regulated DEGs were calculated from GSE148994. As for GSE149055, there were 1068 up-regulated and 3913 down-regulated DEGs. Heat map of DEGs in each dataset was shown in Figure 1C, D and E. The DEGs in each group were mixed by the Venn plot. From the Venn polt shown in Figure 1A and B, there were 824 common DEGs among the three subgroups, of which 350 were up-regulated DEGs and 474 were down-regulated.

Protein-protein interaction (PPI) network construction and sub-modules

824 notes and 3200 edges consist the full network shown in Figure 2A. Meanwhile, with the aid of the MCOD app, top 3 modules were selected and shown in Figure 2B,C,D with 28 notes and 349 edges in module 1, 36 notes and 237 edges in module 2 and 47 note notes and 176 edges in modules 3.From the MCOD function, 19 hub genes were selected: ASXL1, BOC, CENPH, DIMT1, ESRP1, GLDC, HOXD3, IGFBP5, JUN, MGST1, MRPS34, MSTN, MYOD1, MYOG, NBAS, PLS1, POLR3G, RNF144B, UST.

GO and pathway enrichment analysis from the DEGs

The GO analysis was processed to determine the function distributions of common DEGs from three aspect. Figure3a, b and c showed up-regulated DEGs enrichment including KEGG pathways, molecular function (MF), biological processes (BP) and cell composition (CC). In KEGG analysis, the top 3 enriched pathways were pathway in cancer, PI3K pathway, actin cytoskeleton regulation. DEGs were enrich in transcription functions in BP, extra-celluar communications in CC and DNA binding in MF. Meanwhile, the down-regulated DEGs showed in Figure 4a, b and c mainly distributed in metabolic pathway, biosynthesis of antibodies and cell cycle. In the up-regulated function analysis, from BP to CC and MF, MYOD1 showed significantly differentially expressed. According to the KEGG analysis, the enriched pathway "actin cytoskeleton regulation" was on the way of myogenic differentiation. The GSEA analysis of DEGs was processed and the results were shown in Figure 5a B and C. The DEGs were enrich in "myogenesis" and "muscle cell development". MyoD1 was "core enrichment" gene in both enriched pathways. Therefore, we set the MyoD1 as the hub gene and "actin cytoskeleton regulation" pathway as the mainly enriched functional pathway.

The expression of ADSCs and BMSCs surface markers

Specific membrane markers confirmed the identity of ADSCs via flow cytometry. According to the results, the ADSCs results are presented in figure 6C, with a strong expression of CD90 at 82.8% positive and weak expression of CD45 at 4.58% positive and the results were shown in Figure6C that the x-axis is the fluorescence intensity, and the y-axis is the cell number.

Cell viability authenticated by MTT

The MTT results were converted into figure6B to show cell viabilities when different concentrations of 5-Aza induced the cells. As is shown in the figure 6B,5-Aza do have does dependent and time dependent toxic effects on ADSCs. As the concentration of 5-Aza increased, the absorbance was significantly decreased. The results revealed that increased concentration of 5-Aza showed increased toxic effects on ADSCs. Meanwhile, when compared with different time-point after induction, the absorbance at 48 hours and 72 hours were significantly decreased when compared to 24 hours after induction. The results revealed that increased induction duration of 5-Aza showed increased toxic effects on ADSCs. It can be calculated that the IC50 in ADSCs groups were 9.178μmol/l at 24hours after induction. The further induce concentration of 5-Aza was set as 0, 10 and 20μmol/l and named as group A, B and C, respectively.

Actin expression determined by immunohistochemistry

The results of the expression of actin were shown in Figure 6D. Actin was labeled and stained red by α-SAM, and the nucleus was stained blue by ho-chest, with the composed pictures showing that there were just parts of the cells expressing actin. The differentiated rate was calculated by graphpad 8.0.2. And the rate of each group was 0.019, 0.074 and 0.116 for groups A, B, and C, respectively. The differentiation rate in group B and C was significantly up-regulated when compared to group A.($P<0.05$)

The content of myoD mRNA measured by RT-PCR

We further used the RT-PCR technology to detect the content of the mRNA of myoD in each group under the induction of 5-Aza. The results were recorded at1.009, 2.391, and 4.876, respectively in each group. Of which the content in group C was significantly up-regulated than group B ($p<0.05$) whose content was also up-regulated compare to group A with significance($P<0.05$).

Discussion

Mountainous efforts have been devoted to the research of pluripotent stem cells in our nowadays research for their regenerating and repairing damaged tissues effects.[18-20] In the musculoskeletal field, the degenerated and decreased of muscle tissue have confused the clinical effects of various diseases.[21, 22] The regeneration and remobilization of degenerated and damaged muscle tissues have been a hot issue in the research.[23] Stem cells, owning the myogenic differentiation, provide a possibility for current issue. However, the specific key pathways and genes in the myogenesis of stem cells is still under mystic.

There stands various signaling pathways which were count in the myogenic differentiate process of stem cells. Fu, S reported that PI3K pathway related genes and proteins were up-regulated expressed in the myogenic differentiate courses of mouse stem cells[10]. Meanwhile, up-regulated p53 and actin signaling pathways were also proved to be responsible for the myogenesis of stem cells which were certified by Liu, L.[24] and Petschnik, A. E[24]. Except that, p38 signaling pathway and wnt pathway were both proved to be responsible for the process.[25, 26] As for the myogenic genes, MRFs, myoD, myoG, etc[27, 28] were all reported as myogenic related genes.

In the present study, a bioinformatics analysis was used to analysis the key pathways and hub genes in myogenesis of stem cells based on 3 GEO databases. According to the analysis, a total of 824 DEGs were hunted out and applied for the further GO and KEGG analysis to certify potential biological functions and pathways in myogenic differentiation. Except that, 111 genes from the top 3 clusters and 19 hub genes analyzed from the MCODE method were identified from the PPI network.

MyoD has been described as the decisive gene and component of diverting undifferentiated cells into myoblasts[29, 30].Yamamoto M[31]. reported that the muscle satellite cells lacking myoD increased propensity for non-myogenic differentiation and concluded that myoD is a determinate factor that induced the stem cells to muscles. Meanwhile, several researches have shown that myoD play an important role in the myogenic process[32-34]. In Rudnicki[35] research, knock out of myoD and myf5 results in the prevention of formation of skeletal muscle in the embryo period. The study results revealed that myoD and myof5 were determined genes in the origination of muscle cells. In the present bioinformatic analysis, myoD showed key effects in the myogenesis. In GO analysis of up-regulated genes, myoD showed significant in positive regulation of myoblast differentiation in BP, transcription factor complex in CC and chromatin binding, transcription factor binding, transcription factor activity in MF. Meanwhile, the GSEA analysis revealed that moyD were both core enriched elements in myogenesis and muscle cell development in the three GEO databases. The unit results from our analysis revealed that myoD can be one of the hub genes in the myogenic differentiating process. From the laboratory experiments, RT-PCR results revealed that myoD were exactly significantly up-regulated in myogenic induced stem cells.

Also, we performed KEGG analysis to trace out the exact relevant pathways in the myogenic differentiation not only in the DEGs, but also based on the intensive module analysis from the PPI network. From the DEGs, the activation of PI3K, actin cytoskeleton regulation, p53 signaling pathway were proved to be tightly associated with myogenesis process. Meanwhile, the intensive analysis showed that actin cytoskeleton regulation pathway was also enriched. Panagiotis M[36] recovered the myogenic differentiation potential by restoring the actin organization which revealed that actin is necessary in the myogenic differentiation. Anna E[27] found myogenic differentiating abilities in glandular stem cells who owns the actin expression. Actin have been a widely spread method to determine the myogenesis in various research[37-39]. But few researches have devoted to determine the specific time-point for the expression of actin during the myogenic differentiation process. Based on our laboratory experiments, the expression of actin was exactly significantly up-regulated in myogenic induced stem cells.

The study still has several limitations. Firstly, the included GEO profiles were still not rich enough. Secondly, the specific genes regulations in different time point of differentiation were omitted in our study. We still need to conduct further validate experiment to proof our speculation in the future.

Conclusion

Our study identified a series of DEGs in the myogenic differentiation process compared to undifferentiated stem cells. The 19 hub genes ASXL1, BOC, CENPH, DIMT1, ESRP1, GLDC, HOXD3, IGFBP5, JUN, MGST1, MRPS34, MSTN, MYOD1, MYOG, NBAS, PLS1, POLR3G, RNF144B, UST were selected from the series bioinformatics analysis. From the further GO and KEGG analysis, the pathways own enriched genes were selected. Our analysis revealed the hub genes and key pathways in the myogenic differentiation process of stem cells.

Declarations

Ethics approval and consent to participate

This study was approved by ethics of committee of Northern Jiangsu People's Hospital.

Consent for publish

Not applicable.

Availability of data and materials

The data used and analyzed during the current study are available from the corresponding author on reasonable request.

Competing Interest

The authors declare that they have no competing interests.

Funding:

This work was supported by the funds from the young medical key talent project of Jiangsu province (contract number QNRC2016458). Jiangsu Provincial Medical Innovation Team (Grant#CXTDB2017004).

Authors' contributions

Wenyong Fei, Mingsheng Liu and Jingcheng Wang: conception and design, financial support, experiment, manuscript writing, final approval of manuscript.

Mingsheng Liu made the equal contribution to the article and should be considered co-first author. Correspondence: Jingcheng Wang.

Yao Zhang,Shichao Cao, Xuanqi Wang, Bin Xie:analysis and interpretation of data and drafted the manuscript.

All authors read and approved the final manuscript.

References

1. André, L.M., et al., *Abnormalities in Skeletal Muscle Myogenesis, Growth, and Regeneration in Myotonic Dystrophy.* Front Neurol, 2018. **9**: p. 368.
2. Rajasekaran, M.R., et al., *Age and multiparity related urethral sphincter muscle dysfunction in a rabbit model: Potential roles of TGF-β and Wnt-β catenin signaling pathways.* Neurourol Urodyn, 2019. **38**(2): p. 607-614.
3. Biltz, N.K., et al., *Infiltration of intramuscular adipose tissue impairs skeletal muscle contraction.* J Physiol, 2020. **598**(13): p. 2669-2683.
4. Phung, L.A., et al., *Age affects myosin relaxation states in skeletal muscle fibers of female but not male mice.* PLoS One, 2018. **13**(9): p. e0199062.
5. White, Z., et al., *High prevalence of plasma lipid abnormalities in human and canine Duchenne and Becker muscular dystrophies depicts a new type of primary genetic dyslipidemia.* J Clin Lipidol, 2020.
6. Lee, J.K., et al., *Comparison of Bone Mineral Density and Appendicular Lean Body Mass between Osteoporotic Distal Radius Fracture and Degenerative Rotator Cuff Tear in Women Patients.* J Bone Metab, 2017. **24**(4): p. 235-240.
7. Narvani, A.A., et al., *Degenerative rotator cuff tear, repair or not repair? A review of current evidence.* Ann R Coll Surg Engl, 2020. **102**(4): p. 248-255.
8. Krawczenko, A., et al., *Microvesicles from Human Immortalized Cell Lines of Endothelial Progenitor Cells and Mesenchymal Stem/Stromal Cells of Adipose Tissue Origin as Carriers of Bioactive Factors Facilitating Angiogenesis.* Stem Cells Int, 2020. **2020**: p. 1289380.
9. Sadeghi, Z., et al., *Transcriptomic Analysis of Human Mesenchymal Stem Cell Therapy in Incontinent Rat Injured Urethra.* Tissue Eng Part A, 2020.
10. Li, P., et al., *Effects of local injection and intravenous injection of allogeneic bone marrow mesenchymal stem cells on the structure and function of damaged anal sphincter in rats.* J Tissue Eng Regen Med, 2020.
11. Osborn, D.P.S., et al., *Fgf-driven Tbx protein activities directly induce myf5 and myod to initiate zebrafish myogenesis.* Development, 2020. **147**(8).
12. Skrzypek, K., et al., *SNAIL is a key regulator of alveolar rhabdomyosarcoma tumor growth and differentiation through repression of MYF5 and MYOD function.* Cell Death Dis, 2018. **9**(6): p. 643.
13. Zammit, P.S., *Function of the myogenic regulatory factors Myf5, MyoD, Myogenin and MRF4 in skeletal muscle, satellite cells and regenerative myogenesis.* Semin Cell Dev Biol, 2017. **72**: p. 19-32.

14. Huang, W., et al., *The Inhibition on MDFIC and PI3K/AKT Pathway Caused by miR-146b-3p Triggers Suppression of Myoblast Proliferation and Differentiation and Promotion of Apoptosis.* Cells, 2019. **8**(7).
15. Zhang, K., et al., *Islr regulates canonical Wnt signaling-mediated skeletal muscle regeneration by stabilizing Dishevelled-2 and preventing autophagy.* Nat Commun, 2018. **9**(1): p. 5129.
16. Kobatake, K., et al., *Kdm6a Deficiency Activates Inflammatory Pathways, Promotes M2 Macrophage Polarization, and Causes Bladder Cancer in Cooperation with p53 Dysfunction.* Clin Cancer Res, 2020. **26**(8): p. 2065-2079.
17. Kowalski, K., et al., *Stem cells migration during skeletal muscle regeneration - the role of Sdf-1/Cxcr4 and Sdf-1/Cxcr7 axis.* Cell Adh Migr, 2017. **11**(4): p. 384-398.
18. Jinno, H., *Regeneration using endogenous neural stem cells following neonatal brain injury.* Pediatr Int, 2020.
19. Wang, Y., U. Armato, and J. Wu, *Targeting Tunable Physical Properties of Materials for Chronic Wound Care.* Front Bioeng Biotechnol, 2020. **8**: p. 584.
20. Yao, J., Y. Yu, and S.L. Nyberg, *Induced Pluripotent Stem Cells for the Treatment of Liver Diseases: Novel Concepts.* Cells Tissues Organs, 2020: p. 1-17.
21. Fariyike, B., et al., *Role of MicroRNA-141 in the Aging Musculoskeletal System: A Current Overview.* Mech Ageing Dev, 2019. **178**: p. 9-15.
22. Roberts, S., et al., *Ageing in the musculoskeletal system.* Acta Orthop, 2016. **87**(sup363): p. 15-25.
23. Nancarrow-Lei, R., et al., *A Systemic Review of Adult Mesenchymal Stem Cell Sources and their Multilineage Differentiation Potential Relevant to Musculoskeletal Tissue Repair and Regeneration.* Curr Stem Cell Res Ther, 2017. **12**(8): p. 601-610.
24. Liu, L., et al., *Impaired Notch Signaling Leads to a Decrease in p53 Activity and Mitotic Catastrophe in Aged Muscle Stem Cells.* Cell Stem Cell, 2018. **23**(4): p. 544-556.e4.
25. Segalés, J., E. Perdiguero, and P. Muñoz-Cánoves, *Regulation of Muscle Stem Cell Functions: A Focus on the p38 MAPK Signaling Pathway.* Front Cell Dev Biol, 2016. **4**: p. 91.
26. Ye, X., et al., *Irisin reverses insulin resistance in C2C12 cells via the p38-MAPK-PGC-1α pathway.* Peptides, 2019. **119**: p. 170120.
27. Petschnik, A.E., et al., *The role of alpha-smooth muscle actin in myogenic differentiation of human glandular stem cells and their potential for smooth muscle cell replacement therapies.* Expert Opin Biol Ther, 2010. **10**(6): p. 853-61.
28. Jin, C., et al., *A Lipid-Nanosphere-Small MyoD Activating RNA-Bladder Acellular Matrix Graft Scaffold [NP(saMyoD)/BAMG] Facilitates Rat Injured Bladder Muscle Repair and Regeneration [NP(saMyoD)/BAMG].* Front Pharmacol, 2020. **11**: p. 795.
29. Davis, R.L., H. Weintraub, and A.B. Lassar, *Expression of a single transfected cDNA converts fibroblasts to myoblasts.* Cell, 1987. **51**(6): p. 987-1000.

30. Kim, J.A., et al., *MYOD mediates skeletal myogenic differentiation of human amniotic fluid stem cells and regeneration of muscle injury.* Stem Cell Res Ther, 2013. **4**(6): p. 147.
31. Yamamoto, M., et al., *Loss of MyoD and Myf5 in Skeletal Muscle Stem Cells Results in Altered Myogenic Programming and Failed Regeneration.* Stem Cell Reports, 2018. **10**(3): p. 956-969.
32. Zhang, F., et al., *PPARγ and MyoD are differentially regulated by myostatin in adipose-derived stem cells and muscle satellite cells.* Biochem Biophys Res Commun, 2015. **458**(2): p. 375-80.
33. Sung, S.E., et al., *MyoD Overexpressed Equine Adipose-Derived Stem Cells Enhanced Myogenic Differentiation Potential.* Cell Transplant, 2016. **25**(11): p. 2017-2026.
34. Patruno, M., et al., *Tat-MyoD fused proteins, together with C2c12 conditioned medium, are able to induce equine adult mesenchimal stem cells towards the myogenic fate.* Vet Res Commun, 2017. **41**(3): p. 211-217.
35. Megeney, L.A. and M.A. Rudnicki, *Determination versus differentiation and the MyoD family of transcription factors.* Biochem Cell Biol, 1995. **73**(9-10): p. 723-32.
36. Mistriotis, P., et al., *NANOG Reverses the Myogenic Differentiation Potential of Senescent Stem Cells by Restoring ACTIN Filamentous Organization and SRF-Dependent Gene Expression.* Stem Cells, 2017. **35**(1): p. 207-221.
37. Nazari, M., et al., *Mast cells promote proliferation and migration and inhibit differentiation of mesenchymal stem cells through PDGF.* J Mol Cell Cardiol, 2016. **94**: p. 32-42.
38. Molony, C., et al., *Label-free discrimination analysis of de-differentiated vascular smooth muscle cells, mesenchymal stem cells and their vascular and osteogenic progeny using vibrational spectroscopy.* Biochim Biophys Acta Mol Cell Res, 2018. **1865**(2): p. 343-353.
39. Helms, F., et al., *Complete Myogenic Differentiation of Adipogenic Stem Cells Requires Both Biochemical and Mechanical Stimulation.* Ann Biomed Eng, 2020. **48**(3): p. 913-926.

Figures

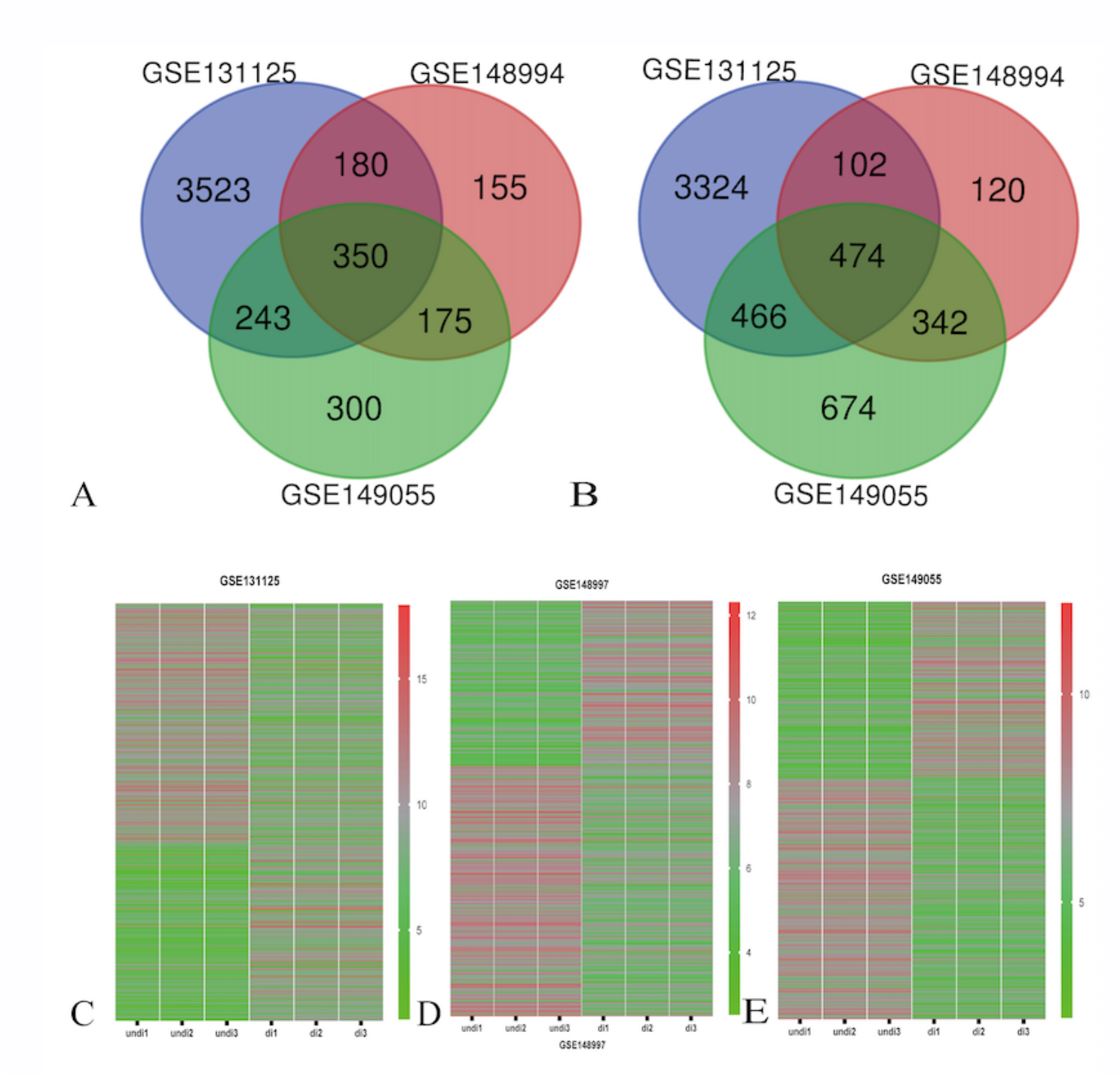

Figure 1

A. Venn diagram of up-regulated DEGs across different profiles. B.Venn diagram of up-regulated DEGs across different profiles. C. Heat map of DEGs in GSE131125, D. Heat map of DEGs in GSE 148994, E. Heat map of DEGs in GSE140955

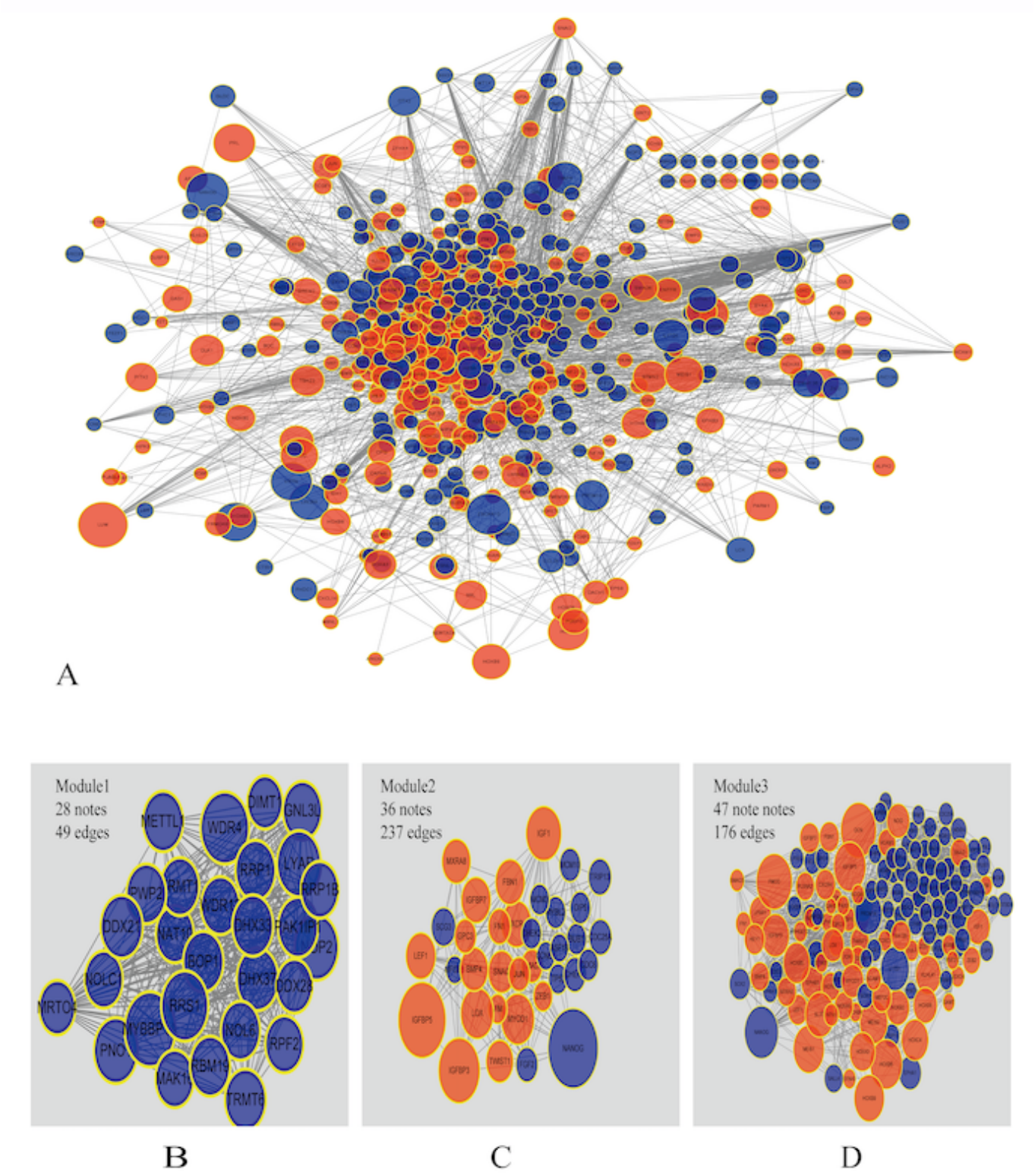

Figure 2

A.Protein-protein interaction (PPI) network construction. A total of 824 DEGs were identified as hub genes B. C. D: The significant top 3 modules in the PPI network. Genes with blue represent down-regulated hub genes and with red represent up-regulated genes. The size of each gene was based on the interaction analysis that bigger size indicate more interactions.

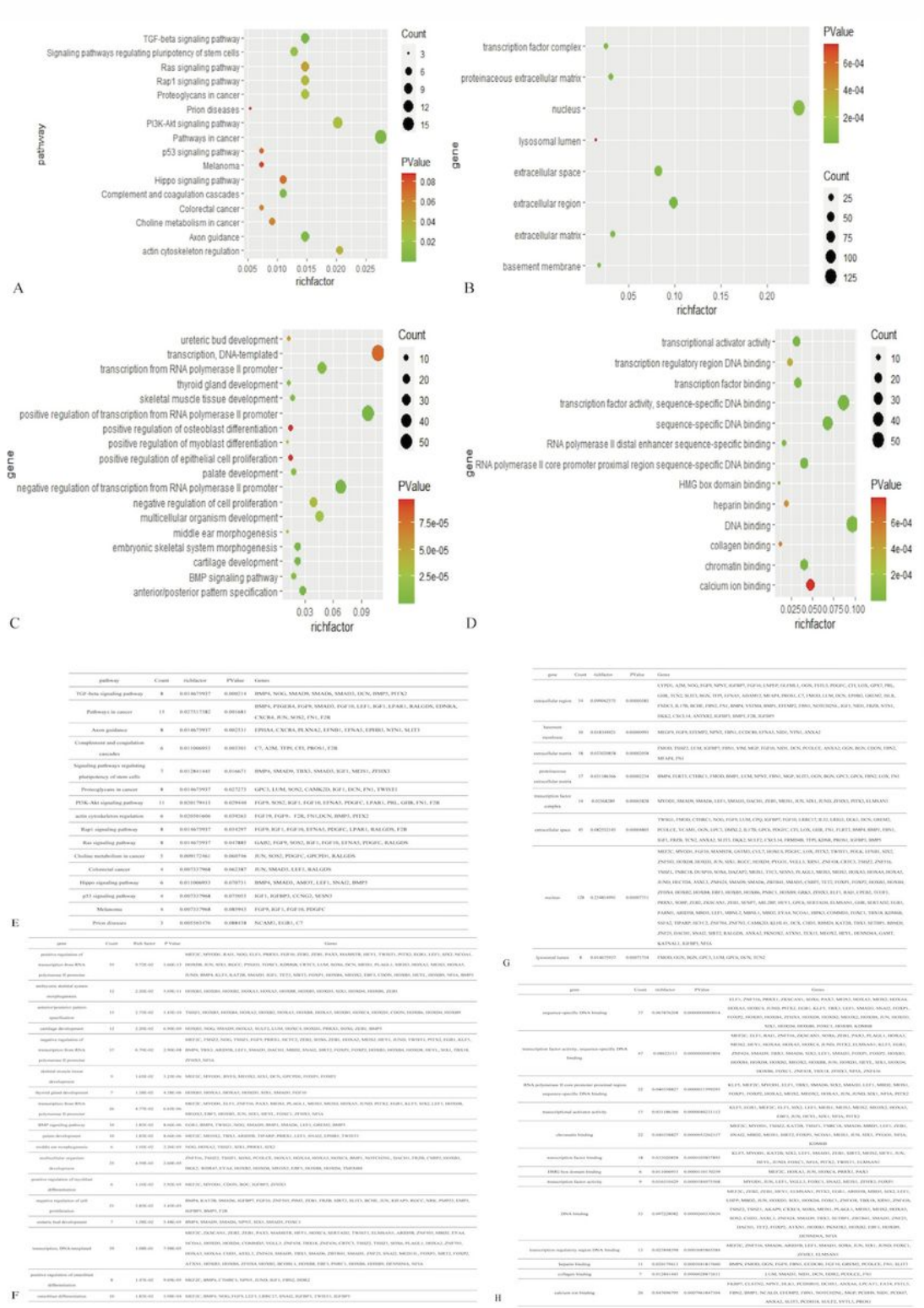

Figure 3

3a: Bubble diagram of KEGG pathway analysis and GO analysis of up-regulated genes. A. KEGG analysis of up-regulated genes. B. CC functional classification terms of up-regulated genes. C. BP functional classification terms of up-regulated genes. D. MF functional classification terms of up-regulated genes. 3b: GO analysis and KEGG analysis based on up-regulated genes. E.Individual KEGG terms and their corresponding genes in each group. F. Top BP terms and their corresponding genes in GO functional

analyses 3c: GO analysis and KEGG analysis based on up-regulated genes. G. Top CC terms and their corresponding genes in GO functional analysis. H.Top CC terms and their corresponding genes in GO functional analysis

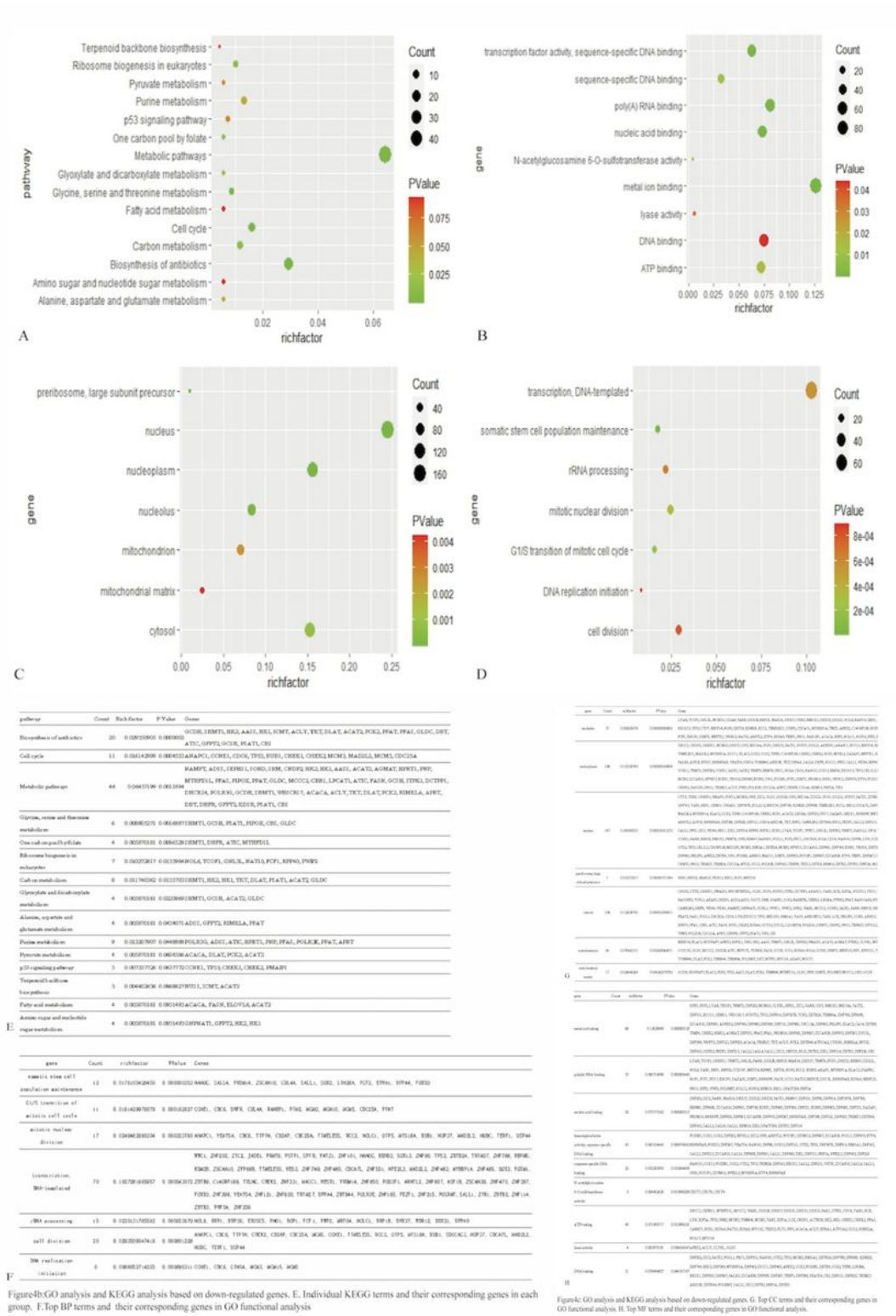

Figure4b:GO analysis and KEGG analysis based on down-regulated genes. E. Individual KEGG terms and their corresponding genes in each group. F.Top BP terms and their corresponding genes in GO functional analysis

Figure4c: GO analysis and KEGG analysis based on down-regulated genes. G. Top CC terms and their corresponding genes in GO functional analysis. H. Top MF terms and their corresponding genes in GO functional analysis.

Figure 4

4a: Bubble diagram of KEGG pathway analysis and GO analysis of down-regulated genes. A. KEGG analysis of down-regulated genes. B. MF functional classification terms of down-regulated genes. C. BP

functional classification terms of down-regulated genes. D. CC functional classification terms of down-regulated genes. 4b: GO analysis and KEGG analysis based on down-regulated genes. E. Individual KEGG terms and their corresponding genes in each group. F.Top BP terms and their corresponding genes in GO functional analysis 4c: GO analysis and KEGG analysis based on down-regulated genes. G. Top CC terms and their corresponding genes in GO functional analysis. H. Top MF terms and their corresponding genes in GO functional analysis.

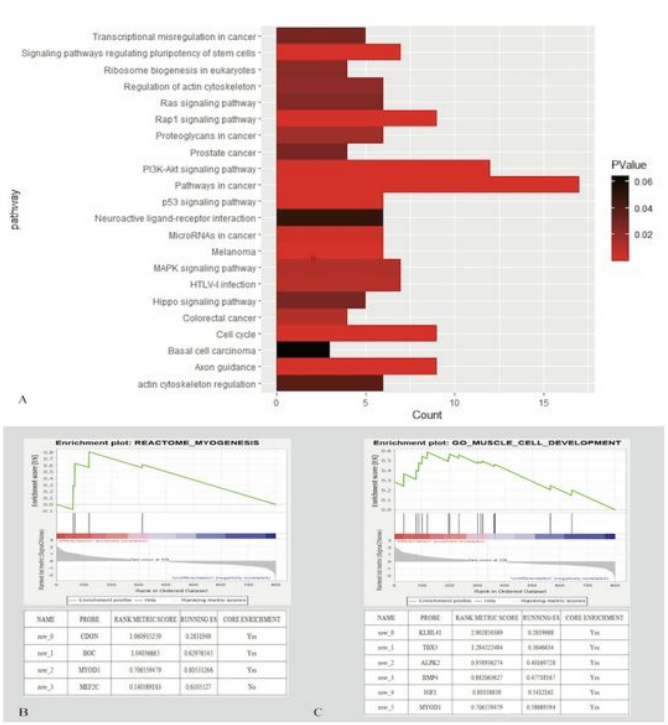

pathway	Count	richfactor	PValue	Genes
Basal cell carcinoma	3	0.015976142	0.064615716	BMP4, TP53, LEF1
Colorectal cancer	4	0.021301523	0.011335678	JUN, TP53, SMAD3, LEF1
Ribosome biogenesis in eukaryotes	4	0.021301523	0.022614833	NOL6, NAT10, GNL3L, PWP2
Prostate cancer	4	0.021301523	0.029043774	CCNE1, TP53, LEF1, IGF1
Hippo signaling pathway	5	0.026626904	0.028405928	BMP4, SOX2, SMAD3, LEF1, SNAI2
Transcriptional misregulation in cancer	5	0.026626904	0.029011191	MEF2C, TP53, IGF1, MEIS1, IGFBP3
p53 signaling pathway	6	0.031952285	1.30E-04	CCNE1, TP53, IGF1, CHEK1, CHEK2, IGFBP3
Melanoma	6	0.031952285	1.98E-04	FGF19, FGF9, TP53, FGF10, IGF1, FGF2
actin cytoskeleton regulation	6	0.020501606	0.039263	FGF19, FGF9，F2R, FN1, DCN, BMP5, PITX2
MicroRNAs in cancer	6	0.031952285	0.004118027	CCNE1, VIM, TP53, ZEB2, ZEB1, CDC25A
Proteoglycans in cancer	6	0.031952285	0.016548918	NANOG, GPC3, TP53, IGF1, FGF2, FN1
Regulation of actin cytoskeleton	6	0.031952285	0.02167309	FGF19, FGF9, FGF10, FGF2, F2R, FN1
Ras signaling pathway	6	0.031952285	0.025463613	FGF19, FGF9, FGF10, IGF1, EFNA5, FGF2
Neuroactive ligand-receptor interaction	6	0.031952285	0.050711809	EDNRA, CCKBR, GRPR, LPAR3, LPAR1, F2R
Signaling pathways regulating pluripotency of stem cells	7	0.037277665	5.92E-04	BMP4, NANOG, SOX2, SMAD3, IGF1, FGF2, MEIS1
HTLV-I infection	7	0.037277665	0.010614644	VCAM1, EGR1, JUN, TP53, SMAD3, CHEK1, CHEK2
MAPK signaling pathway	7	0.037277665	0.011443862	FGF19, MEF2C, FGF9, JUN, TP53, FGF10, FGF2
Cell cycle	9	0.047928427	3.72E-06	CCNE1, CDC6, BUB1, TP53, SMAD3, CHEK1, CHEK2, MCM3, CDC25A
Axon guidance	9	0.047928427	3.92E-06	EPHA4, CXCR4, PLXNA2, EFNB1, EFNA5, EPHB3, EPHA1, NTN1, SLIT3
Rap1 signaling pathway	9	0.047928427	1.61E-04	FGF19, FGF9, FGF10, LPAR3, IGF1, EFNA5, LPAR1, FGF2, F2R
PI3K-Akt signaling pathway	12	0.063904569	3.90E-05	FGF19, CCNE1, FGF9, TP53, FGF10, LPAR3, IGF1, EFNA5, LPAR1, FGF2, F2R, FN1
Pathways in cancer	17	0.090531473	1.72E-08	BMP4, FGF19, FGF9, TP53, LPAR3, SMAD3, FGF10, IGF1, LEF1, LPAR1, EDNRA, CCNE1, CXCR4, JUN, FGF2, FN1, F2R

Figure 5

5a: KEGG pathway analysis and GSEA analysis based on DEGs. A. Histogram of KEGG pathway analysis of DEGs. B. GSEA analysis of myogenesis pathway and the core genes. C. GSEA analysis of muscle cell development and the core genes. 5b: Individual KEGG terms based on DEGs and their corresponding genes in each group.

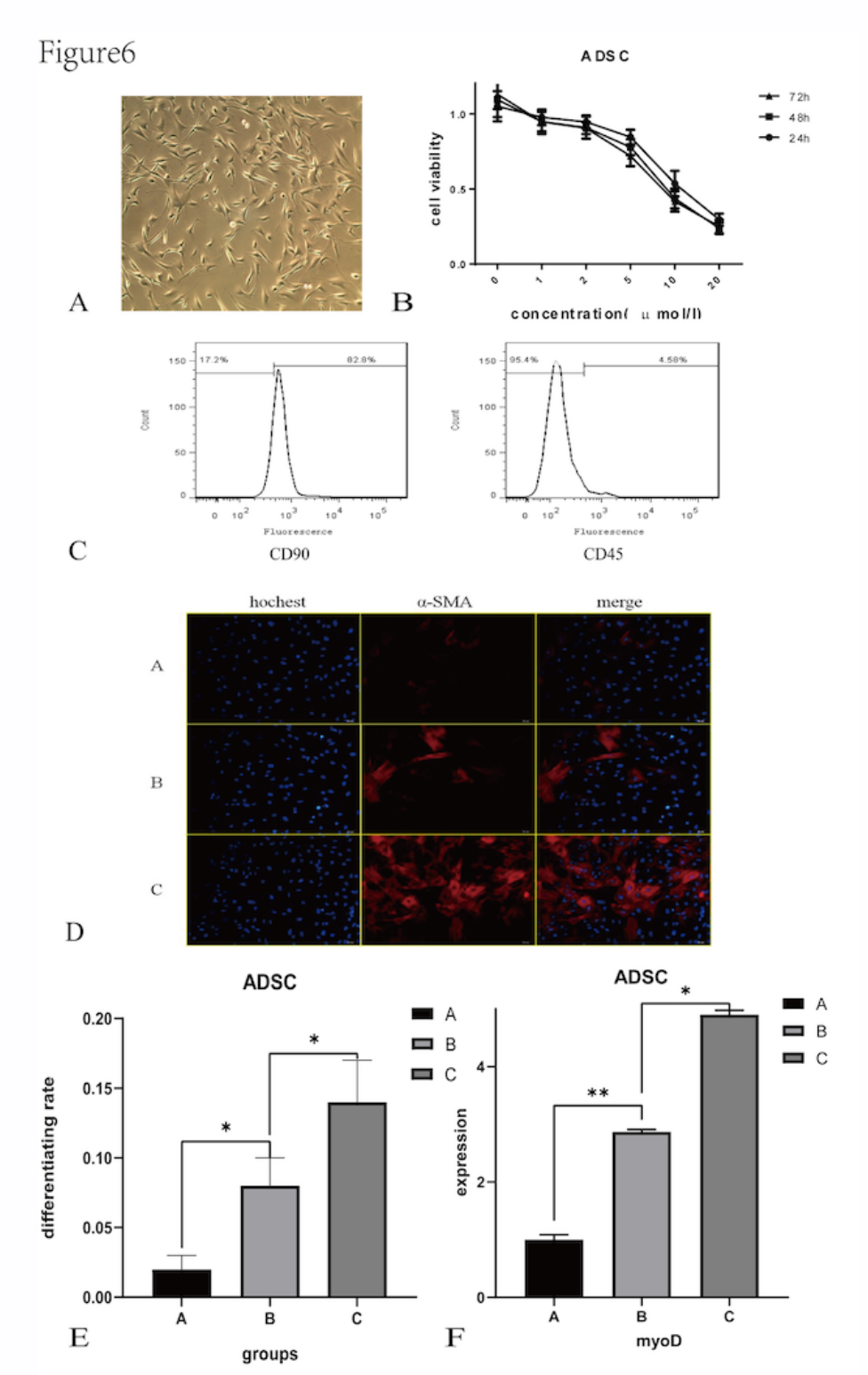

Figure 6

Experimental certification of the hub genes and key pathways. A.Cellular morphology of passage-3 ADSCs. B. MTT assessment showing the effect of different concentrations of 5-Aza on the viability of ADSCs at passage 3 after 1, 3, 5, 7, and 9 days of exposure. The x-axis is the time (days), and the y-axis is the cell viability value . C.Flow cytometry analysis results and expression of cell surface CD markers of ADSCs at passage 3 . The x-axis is the fluorescence intensity, and the y-axis is the cell number.

E.Immunofluorescence analysis of ADSCs. The results represent sarcomeric-a-actinin expression in ADSCs exposed to three myogenic concentration protocols. E.Myogenic differentiation rates are represented by the percent expression of actin as measured by immunohistochemistry. F.MyoD (RT-PCR) mRNA expression levels